# Role of Charged Residues of *pharaonis* Phoborhodopsin (Sensory Rhodopsin II) in Its Interaction with the Transducer Protein[†]

Yuki Sudo, Masayuki Iwamoto, Kazumi Shimono, and Naoki Kamo*

*Laboratory of Biophysical Chemistry, Graduate School of Pharmaceutical Sciences, Hokkaido University, Sapporo 060-0812, Japan*

*Received June 9, 2004; Revised Manuscript Received August 3, 2004*

ABSTRACT: *pharaonis* phoborhodopsin (*p*pR; also called *pharaonis* sensory rhodopsin II, NpSRII) is a receptor for negative phototaxis in *Natronomonas* (*Natronobacterium) pharaonis*. In membranes, it forms a 2:2 complex with its transducer protein, *p*HtrII, which transmits light signals into the cytoplasmic space through protein−protein interactions. We previously found that a specific deprotonated carboxyl of *p*pR or *p*HtrII strengthens their binding [Sudo, Y., et al. (2002) *Biophys. J. 83*, 427−432]. In this study we aim to identify this carboxyl group. Since the D75N mutant has only one photointermediate ($p$pR$_{O-like}$) whose existence spans the millisecond time range, the analysis of its decay rate is simple. We prepared various D75N mutants such as D75N/D214N, D75N/K157Q/R162Q/R164Q (D75N/3Gln), D75N/D193N, and D75N/D193E, among which only D75N/D193N did not show pH dependence with regard to the $p$pR$_{O-like}$ decay rate and $K_D$ value for binding, implying that the carboxyl group in question is from Asp-193. The p$K_a$ of this group decreased to below 2 when a complex was formed. Therefore, we conclude that Asp-193$^{ppR}$ is connected to the distant transducer−*p*pR binding surface via hydrogen bonds, thereby modulating its p$K_a$. In addition, we discuss the importance of Arg-162$^{ppR}$ with respect to the binding activity.

*pharaonis* phoborhodopsin (*p*pR;[1] also called *pharaonis* sensory rhodopsin II, NpSRII) is one of the seven-transmembrane helical retinal proteins that use retinal as a chromophore (*1*−*4*), whereby it binds a specific Lys residue (Lys-205) through a Schiff base linkage. Recently, retinal proteins have been found in various organisms of archaea, eubacteria, and eukaryotes (*5*−*8*). Functionally, these proteins are distinctly classified into two groups: light-driven ion pumps such as bacteriorhodopsin from archaea, which function to pump ions outward (*9*), and photosensors such as *p*pR (for a review see ref *10*). Photosensors form a signaling complex with their own transducer proteins. The photosensor protein *p*pR binds with the *pharaonis* halobacterial transducer protein *p*HtrII in the membrane.

*p*HtrII is a two-transmembrane helical protein that belongs to a family of two-transmembrane helical methyl-accepting chemotaxis proteins (MCPs) (*11*, *12*). MCP exists as a homodimer composed of a 50−60 kDa subunit and forms a ternary complex with CheA and CheW. Chemical stimuli activate phosphorylation cascades that modulate flagellum motors (*13*−*15*). For chemoreception in bacteria, MCP acts not only as a chemoreceptor but also as a transducer. On the other hand, for photoreception in archaea, the receptor (e.g., *p*pR) and the transducer (e.g., *p*HtrII) are separated, and direct interaction between them is required (*16*, *17*). *p*pR transmits light signals to *p*HtrII, and this activates phosphorylation cascades that modulate flagellum motors. Using this signaling system, the bacterium can avoid harmful near-UV light, and thus, this process is called negative phototaxis. *p*pR maximally absorbs light at 498 nm, which triggers *trans*−*cis* photoisomerization of the retinal chromophore (*18*). Relaxation of the retinal leads to functional processes during the photocycle. Thus, the active intermediates of the *p*pR/*p*HtrII complex are M- and O-intermediates (*19*).

*p*pR is stable in the membrane and detergent micelles (*20*, *21*), and an expression system using *Escherichia coli* cells can be used to produce large amounts of this protein (*22*). Therefore, *p*pR has been well-characterized over the past few years (*2*, *10*). On the other hand, there has been less progress in the characterization of *p*HtrII. We previously discovered the 1:1 stoichiometry of the *p*pR/*p*HtrII complex and determined its binding constants under various conditions (*23*, *24*). In addition, we showed that the Tyr-199 and Thr-204 residues of *p*pR play roles in its binding with *p*HtrII (*25*, *26*). However, detailed studies on this interaction mechanism have not been conducted.

As previously shown (Figure 5 in ref *25*), the dissociation constant of binding, $K_D$, increases with decreasing pH,

[†] This work was supported in part by a Grant-in-Aid for Scientific Research from the Japanese Ministry of Education, Science, Technology, Sports and Culture, Japan.

* To whom correspondence should be addressed. Phone: +81-11-706-3923. Fax: +81-11-706-4984. E-mail: nkamo@pharm.hokudai.ac.jp.

[1] Abbreviations: DM, *n*-dodecyl β-D-maltoside; IPTG, isopropyl 1-thio-β-galactoside; *p*HtrII, *pharaonis* halobacterial transducer II; *p*HtrIIHis, truncated *p*HtrII expressed from position 1 to position 159, for which a six-His tag is attached to the C-terminus; *p*pR, *pharaonis* phoborhodopsin (*pharaonis* sensory rhodopsin II); 3Gln mutant, *p*pR mutant of D75N/K157Q/R162Q/R164Q in which Asp-75, Lys-157, Arg-162, and Arg-164 are replaced by Asn, Gln, Gln, and Gln, respectively; D75N, *p*pR mutant in which Asp-75 is replaced by Asn; other mutants are similarly signified; D75NHis, D75N mutant whose C-terminus is attached to a six-His tag; $p$pR$_{O-like}$, O-like intermediate of the *p*pR D75N mutant; $K_D$, dissociation constant between *p*pR and *p*HtrII.

10.1021/bi048803c CCC: $27.50 
Published on Web 10/06/2004

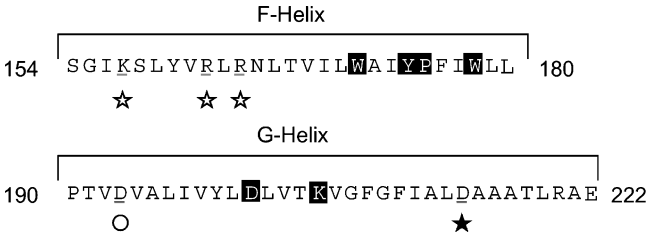


FIGURE 1: Amino acid sequences of helices F and G of *pharaonis* phoborhodopsin (*p*pR) with residues of importance noted. The open circle (Asp-193), closed star (Asp-214), and open star (3Gln) indicate candidates of the carboxyl group whose ionic state may give rise to binding between *p*pR and *p*HtrII. The white letters indicate highly conserved residues among archaeal rhodopsins such as Asp-201 and Lys-205.

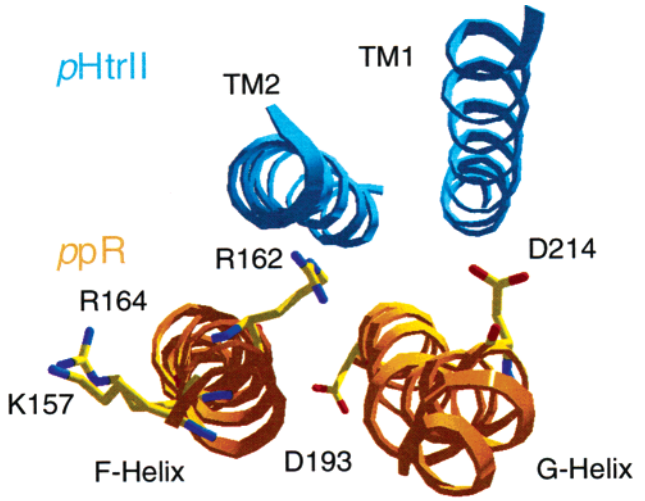


FIGURE 2: X-ray crystallographic structure of the *p*pR/*p*HtrII complex focusing on charged residues of helices F and G of *p*pR. This view is from the cytoplasmic side along the membrane normal. The structure was obtained from the Protein Data Bank (PDB code 1H2S).

meaning that a deprotonated carboxyl(s) of *p*pR or *p*HtrII increases the interaction between *p*pR and *p*HtrII. The relationship between pH and $K_D$ is well-correlated with the Henderson−Hasselbach equation with a p$K_a$ of 3.9. However, the origin of this phenomenon is unknown. In the present study we aim to identify this carboxyl group using mutant proteins. Figure 1 shows the gene sequence of *p*pR for only the helix F and G regions, which are located at the transducer binding surface (*17*). The Asp-214 residue of *p*pR is only the carboxylic residue present in helix F or G that projects toward *p*HtrII (Figure 2). In this regard, the first candidate is the carboxyl group of Asp-214. From the crystal structure of transducer-free *p*pR, Royant et al. (*27*) proposed the importance of a charged surface patch (Lys-157, Arg-162, and Arg-164) on the cytoplasmic side of *p*pR for the interaction with *p*HtrII (Figure 2). This patch does not exist in other archaeal rhodopsins such as bacteriorhodopsin and halorhodopsin. A second candidate is the carboxyl group (Asp-102, Asp-104, and Asp-106 in *p*HtrII) that interacts with the positively charged patch. For the third candidate, the p$K_a$ of the carboxyl group of Asp-193 in helix G of *p*pR decreases when *p*pR binds to *p*HtrII (*28*), suggesting that structural changes occur around Asp-193. Thus, this candidate is the carboxyl group of Asp-193, although it is orientated toward the interior of *p*pR and not toward *p*HtrII (Figure 2). The residue corresponding to Asp-193 in *p*pR is conserved as Glu-204 in bacteriorhodopsin (bR), which is an important residue for proton release (*29*−*33*).

The results of this study rule out the first and second candidates, and suggest that Asp-193 is the residue responsible for binding. Here, we used various D75N mutants of *p*pR because they lack an M-intermediate, and the O-like intermediate *p*p$R_{O-like}$ has the only observable decay rates that can be easily measured by flash photolysis in the millisecond time range. The rate constants are affected by binding, which enabled us to estimate $K_D$ for the binding of various *p*pR mutants to *p*HtrII.

## MATERIALS AND METHODS

*Sample Preparations.* Expression plasmids of D75NHis and *p*HtrIIHis were constructed as previously described (*24*, *34*). Here, His denotes a tag with six histidine residues attached at the C-terminus of the protein. Truncated *p*HtrII expressed from position 1 to position 159 was used instead of the whole protein because the truncated transducer is enough to permit interaction with *p*pR (*35*). Hereafter, *p*HtrII signifies the truncated protein. The mutant genes D75N/D214N, D75N/K157Q/R162Q/R164Q (called mutant 3Gln hereafter), D75N/D193N, and D75N/D193E were constructed by PCR using the QuickChange method. Oligonucleotide primers were designed from nucleotide sequences in the GenBank database (accession no. Z35086), and DNA was sequenced using a DNA sequencing kit (Applied Biosystems). All constructed plasmids were analyzed using an automated sequencer (377 DNA sequencer, Applied Biosystems).

Mutant *p*pRs and *p*HtrII were expressed in *E. coli* BL21 (DE3) cells. The preparation of crude membranes and the purification of proteins were performed as previously described (*36*, *37*). The sample medium was exchanged by ultrafiltration (UK-50, Advantech, Tokyo), and the samples were suspended in media whose compositions will be described later.

For the preparation of the *p*pR/*p*HtrII complex, purified *p*pR and *p*HtrII proteins were mixed in a 1:5 molar ratio followed by incubation for 1 h at 4 °C. Complex formation was confirmed by measuring the decay kinetics of *p*p$R_{O-like}$ and using an in vitro pull-down assay as previously described (*23*, *24*).

*Flash-Photolysis Measurements.* The apparatus and procedure used for flash photolysis were essentially the same as previously described (*38*). The decay of *p*p$R_{O-like}$ of various D75N mutants was observed at 570 nm, and the time courses were analyzed with a single-exponential equation to estimate the kinetic constant. The *p*pR samples were suspended in medium containing 360 mM NaCl, 0.1% *n*-dodecyl $\beta$-D-maltoside (DM), and a mixture of seven buffers (citric acid, Tris, Mes, Hepes, Mops, Ches, and Caps, whose concentrations were 10 mM each), because this buffer has the same buffer capacity over a wide pH range (2−9). Before the flash-photolysis experiments, samples were incubated for at least 1 h in medium whose pH had been adjusted to the required value. All experiments were performed at 20 °C.

*Determination of the Dissociation Constant $K_D$ and the p$K_a$ of An Important Amino Acid Residue from Flash Spectroscopy.* The dissociation constant $K_D$ of various

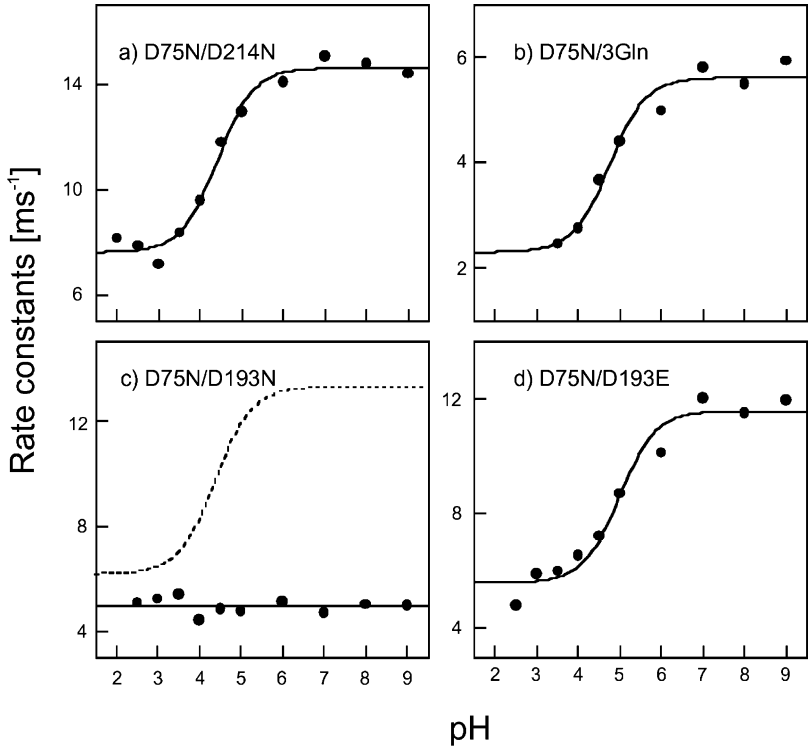


FIGURE 3: Rate constants of *p*pR$_{O-like}$ decay of the transducer-free D75N/D214N (a), D75N/K157Q/R162Q/R164Q or D75N/3Gln (b), D75N/D193N (c), and D75N/D193E (d) mutants. The dashed line in (c) shows data for the D75N mutant from Sudo et al. (*25*). The solid lines are curves fitted using the Henderson−Hasselbach equation with a single p$K_a$ whose values are listed in Table 1. The medium contained a mixture of seven buffers (see the Materials and Methods), 0.1% DM, and 360 mM NaCl, and the experiments were performed at 20 °C.

Table 1: Estimated p$K_a$ Values from the pH Dependence for *p*pR$_{O-like}$ Decay and the Dissociation Constant of the *p*pRD75N/*p*HtrII Complex

| | p$K_a$ (from decay)[a] | p$K_a$ (from $K_D$)[b] | | p$K_a$ (from decay)[a] | p$K_a$ (from $K_D$)[b] |
|---|---|---|---|---|---|
| D75N | 4.4[c] | 3.9[c] | D75N/D193E | 5.0 | 4.7 |
| D75N/D214N | 4.4 | 4.1 | D75N (complex) | <2 | *e* |
| D75N/3Gln[d] | 4.7 | 4.1 | D75N/D193E (complex) | 3.5 | *e* |
| D75N/D193N | ND | ND | | | |

[a] pH-dependent decay rate constants are shown in Figures 3 and 4, from which p$K_a$ values were determined. [b] $K_D$ values are shown in Figure 5 as a function of pH, from which p$K_a$ values were determined. [c] From Sudo et al. (*25*). ND means not determined because of no pH dependence. [d] 3Gln denotes the mutant K157Q/R162Q/R164Q. [e] This value was not determined because the results shown in Figure 4 were obtained in the presence of high enough concentrations of *p*HtrII to prevent dissociation of the complex.

*p*pRD75N/*p*HtrII complexes was determined from the rate constant under varying ratios of *p*pR mutant and *p*HtrII as previously described (*23*): The *p*HtrII concentration was kept constant at 25 $\mu$M, and varying concentrations of *p*pR mutant were added to change the molar ratio of *p*HtrII to the mutant. The *p*HtrII concentration was determined using SDS−PAGE as previously described (*23, 24*).

The determination of $K_D$ was performed at various pH values. Thus, we obtained the relationship for $K_D$ vs pH, and the experimental curves were fitted by the Henderson−Hasselbach equation with a single p$K_a$.

## RESULTS

*Decay Rate Constant of the O-like Intermediate pp$R_{O-like}$.* D75N lacks an M-intermediate during the photocycle because Asp-75, the proton acceptor from the protonated Schiff base, is replaced by a neutral Asn (*39, 41*). A phototransient that maximally absorbs at 570 nm is only observable over the millisecond time range, which we call an O-like intermediate (*p*pR$_{O-like}$) due to the red-shifted absorbance maximum. Using a single-exponential decay equation, we were able to estimate the kinetic decay constants of *p*pR$_{O-like}$. Absorption maxima of the intermediate of all mutants used were not changed by binding to *p*HtrII, and these values were essentially equal to that of D75N alone or its complex, whose values were previously reported (*24*). Figure 3 shows plots of the decay constants versus pH for various *p*pR D75N mutants. We previously found that the rate constants of the transducer-free D75N showed a marked pH dependence, which is delineated by the dashed line in Figure 3c (*25*). Analysis of this curve with the Henderson−Hasselbach equation gave a p$K_a$ of 4.4. The pH dependence of the rate constants was also observed for the D75N/D214N and D75N/3Gln mutants. The p$K_a$ values for these pH dependencies are listed in Table 1, and are almost equal to that of D75N. On the other hand, for the D75N/D193N mutant the pH dependence disappeared, while for the D75N/D193E mutant the pH dependence remained and the p$K_a$ was shifted to 5.0 from 4.4 (the dashed line in Figure 3c and Table 1) due to the replacement of Asp with Glu at position 193 in the D75 mutant. From these results, we identified the carboxyl group

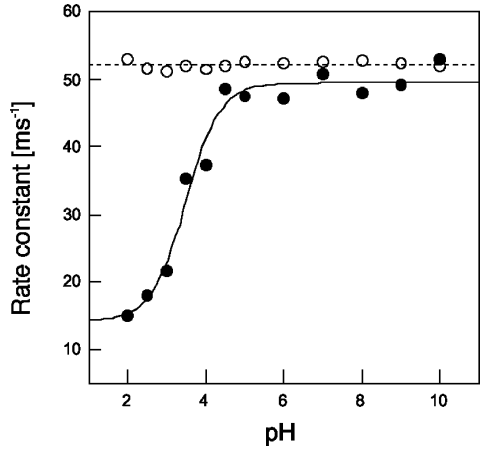


FIGURE 4: Rate constants of *p*pR$_{O-like}$ decay of the D75N/*p*HtrII (open circles) and D75N/D193E/*p*HtrII (closed circles) complexes at various pH values. The solid lines are curves fitted using the Henderson−Hasselbach equation with a single p$K_a$ estimated to be 3.5. The experimental conditions were the same as those in Figure 3. The experiments were performed in the presence of a high enough concentration of *p*HtrII compared to that of *p*pR to prevent the dissociation. For details, see the text.

from Asp-193 as that which is responsible for the pH dependence of the decay rate of *p*pR$_{O-like}$. In comparing the solid and dashed lines in (c), Figure 3 reveals that the deprotonated state of Asp-193 facilitates the decay of *p*pR$_{O-like}$.

Figure 4 shows the decay rate constants of *p*pR$_{O-like}$ of D75N in the presence of *p*HtrII (the *p*pRD75N/*p*HtrII complex) for various pH values. These experiments should be performed in the presence of a high enough concentration of *p*HtrII (above the $K_D$ value; see Figure 5) so that dissociation of the complex does not occur. As described in the Materials and Methods, titration of *p*pR against 25 $\mu$M *p*HtrII was performed, for which *p*pR$_{O-like}$ decay rates were measured at every pH. One or two data points from these titration experiments fulfilled the condition of a high enough molecular ratio of *p*HtrII, so that their average values could be plotted. A comparison with the rate constants of D75N*p*pR alone (the dashed line in Figure 3) indicated the acceleration of *p*pR$_{O-like}$ decay of the *p*pRD75N/*p*HtrII complex. The decay constant of the *p*pRD75N/*p*HtrII complex was not affected over a pH range of 2−10. On the other hand, D75N/D193E/*p*HtrII showed a pH dependence, and decay is faster under the alkaline condition where Glu-193 may have been deprotonated. Hence, Figure 4 together with Figure 3 suggests that the p$K_a$ of Asp-193 of the *p*pRD75N/*p*HtrII complex is lower than 2. Another possibility is that *p*HtrII covers Asp-193 so that this residue is insulated from the external milieu, although the X-ray crystal structure does not support this hypothesis (Figure 2). This can be ruled out because the D75N/D193E/*p*HtrII complex showed a pH dependence, indicating that position 193 may make contact with the external milieu. Analysis of this curve gave a p$K_a$ value of 3.5. However, the p$K_a$ of this glutamic acid is 5.0 in the free state (Table 1), indicating that binding with *p*HtrII decreases the p$K_a$ of the carboxyl group at this position. Therefore, we concluded that association with *p*HtrII decreases the p$K_a$ of Asp-193 of D75N in the *p*pR$_{O-like}$ state to less than 2 from 4.4.

Table 2: Dissociation Constants ($K_D$) and the Number of Binding Sites ($n$) of Complexes of Various *p*pRD75N Mutants and pHTrII in the *p*PR$_{O-like}$ State

| | $K_D$[a] ($\mu$M) | $n$ | | $K_D$[a] ($\mu$M) | $n$ |
|---|---|---|---|---|---|
| D75N[b] | 0.15 | 1.0 | D75N/D193N | 0.67 | 1.0 |
| D75N/D214N | 0.32 | 1.1 | D75N/D193E | 0.99 | 0.9 |
| D75N/3Gln | 9.5 | 1.0 | | | |

[a] The $K_D$ values are those at pH 7.0, which were taken from Figure 5. [b] Data were also taken from a study by Sudo et al. (*24*).

*Estimation of the Dissociation Constant $K_D$ of the Complex between Various D75N Mutants and pHtrII in the pp$R_{O-like}$ State.* We titrated 25 $\mu$M *p*HtrII with various D75N*p*pR mutants to measure the decay rate constants of *p*pR$_{O-like}$, and eight kinetic traces were obtained under different molar ratios of *p*HtrII to *p*pR for each *p*pR mutant. From these data, $K_D$ values were estimated (for details, see refs *23* and *24*). In Figure 5, the $K_D$ values of various D75N mutants are plotted over a pH range between 2 and 9. Table 2 lists the stoichiometric ratio and $K_D$ value at pH 7, where binding was stronger than that in acidic media (Figure 5). These $K_D$ values are similar to that of the complex between the wild-type *p*pR and *p*HtrII in the dark (0.16 $\mu$M) previously reported by Hippler-Mreyen et al. (*35*) except for D75N/3Gln. Due to the low protein stability of the D75N/3Gln, D75N/D193E, and D75N/D193N mutants, it was difficult to measure the decay rate constants and binding parameters under acidic conditions.

As previously described (*25*), the p$K_a$ determined from a plot of $K_D$ vs pH for the D75N/*p*HtrII complex in the *p*pR$_{O-like}$ state is 3.9. For D75N/D193E, the p$K_a$ shifted to 4.7. The pH dependence of $K_D$ exists for D75N/D214N and D75N/3Gln mutants, as shown in Figure 5, although the p$K_a$ is a little larger than 3.9 (see Table 1). D75N/D193N did not show any pH dependence, and the $K_D$ value for the acidic region was almost the same as that of D75N (Figure 5c). These binding analyses suggest that the carboxyl group of *p*pR responsible for the pH dependence of binding (exactly in the *p*pR$_{O-like}$ state) is not that from Asp-214 or the counterions (Asp-102, Asp-104, and Asp-106) of the charged surface patch, but rather the $COO^-$ of Asp-193. Thus, the deprotonated state of Asp-193 in *p*pR (*p*pR$_{O-like}$) plays a role in its interaction with *p*HtrII as well as the pH dependence of the *p*pR$_{O-like}$ decay rate (Figure 3). In Table 1, p$K_a$ values determined from the *p*pR$_{O-decay}$ rate and $K_D$ are listed and are almost equal in value, indicating the importance of the deprotonated (charged) state of Asp-193 for both phenomena.

Table 2 shows that the number of binding sites is almost unity for all complexes, suggesting a 1:1 stoichiometry for the *p*pRD75N mutant/*p*HtrII complex that is the same as that of the wild-type *p*pR/*p*HtrII complex (*17*, *23*). A large $K_D$ value for the 3Gln (K157K/R162Q/R164Q) mutant was noted, suggesting that one of these three residues may be important for interaction with *p*HtrII in the O-like state. The implications of this will be discussed later.

## DISCUSSION

*Transducer Binding Changes the p$K_a$ of Asp-193 in the pp$R_{O-like}$ State.* From Figure 4, we concluded that association with the transducer changes the p$K_a$ of Asp-193 in the

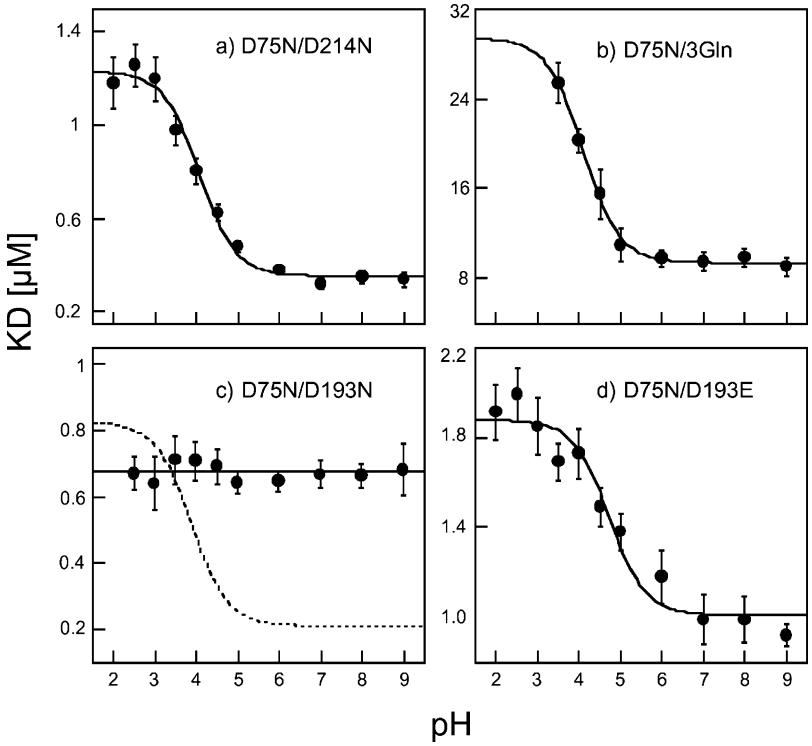


FIGURE 5: $K_D$ values of the D75N/D214N/*p*HtrII (a), D75N/K157Q/R162Q/R164Q/*p*HtrII or D75N/3Gln/*p*HtrII (b), D75N/D193N/*p*HtrII (c), and D75N/D193E/*p*HtrII (d) complexes at various pH values. The dashed line in (c) shows data for the D75N mutant from Sudo et al. (*25*). The solid lines are curves fitted using the Henderson−Hasselbach equation with a single p$K_a$ whose values are listed in Table 1. The experimental conditions were the same as those for Figure 3.

*p*pR$_{O-like}$ state of D75N from 4.4 to <2 (Table 1). This suggests that *p*HtrII binding induces a conformational change around Asp-193, which is located in the extracellular channel and does not face *p*HtrII (Figure 2). We previously reported that a p$K_a$ shift also occurs in the ground state (from 6.4 to 5.6) and the M-intermediate (from 4.9 to 3.9) (*28*) due to complex formation. Bergo et al. (*42*) reported on the effect of transducer binding on the p$K_a$ of an unknown Asp/Glu residue which is deprotonated during the photocycle. According to the crystal structure of the *p*pR/*p*HtrII complex (*17*), the binding surface of *p*pR with *p*HtrII consists of helices F and G, and no essential change in *p*pR occurs due to this association. Nevertheless, a p$K_a$ change was noted in this as well as another study (*28*).

*The Deprotonated State of Asp-193 Increases the Binding Affinity, and Binding Decreases Its p$K_a$.* Using various D75N mutants, we measured the decay rates of *p*pR$_{O-like}$ as well as the $K_D$ values. D75N/D214N, D75N/3Gln, and D75N/D193E showed pH dependence for both constants similar to that of D75N, while D75N/D193N did not show a pH dependence. Therefore, the residue responsible for the pH-dependent dissociation constant is Asp-193. The p$K_a$ values for both are almost equal (Table 1), which indicates that they are regulated by the protonation state of Asp-193. The p$K_a$ of Asp-193 of D75N is 3.9−4.4 (Table 1), and that of the complex is <2 (Table 1 and Figure 4). Thus, schemes for these states are as follows:

for pH > 3.9−4.4

$$\text{D75N}(\text{COO}^{-\,\text{Asp193}}) \text{ at } p\text{pR}_{\text{O-like}} + p\text{HtrII} \leftrightarrow \text{complex}(\text{COO}^{-\,\text{Asp193}}) \; (K_D \approx 0.2\ \mu\text{M})$$

for 2 < pH < 3.9

$$\text{D75N}(\text{COOH}^{\text{Asp193}}) \text{ at } p\text{pR}_{\text{O-like}} + p\text{HtrII} \leftrightarrow \text{complex}(\text{COO}^{-\,\text{Asp193}}) + \text{H}^+ \; (K_D \approx 0.8\ \mu\text{M})$$

The $K_D$ values for this scheme refer to those shown in Figure 5c. When the carboxyl group of Asp-193 is protonated in the free form, the association with *p*HtrII may cause proton release from this residue, which may increase $K_D$. The negatively charged $COO^-$ state of Asp-193 may strengthen the hydrogen bond described below, and thus, the carboxyl group of this residue may be forcibly deprotonated by binding with *p*HtrII. The D75N/D193N mutant forms a complex in which the negative charge cannot be generated due to the replacement of Asp by Asn, and therefore may be a cause of the weak binding (Table 2 and Figure 5).

The X-ray structure shows two hydrogen bonds in the *p*pR/*p*HtrII complex, one between the Tyr-199 residue of *p*pR and Asn-74 residue of *p*HtrII, and the other associated with the Thr-189 residue of *p*pR interacting with the Ser-62 and Glu-43 residues of *p*HtrII. Asp-193$^{ppR}$ also forms a hydrogen bond with Thr-189$^{ppR}$ (Figure 6). It was previously discovered that Thr-189$^{ppR}$ participates in the interaction with *p*HtrII in the ground state (Yamabi et al., manuscript in preparation). It is thus feasible that binding with the transducer changes the degree of hydrogen bonding around Asp-193$^{ppR}$ through the hydrogen-bonding network among Thr-189$^{ppR}$, Ser-62$^{pHtrII}$, and Glu-43$^{pHtrII}$. This hydrogen bonding may result in a decrease in the p$K_a$ of Asp-193 in the binding state (see the above scheme), although Asp-193 is located inside the protein and thus does not appear to directly interact with *p*HtrII (Figure 2).

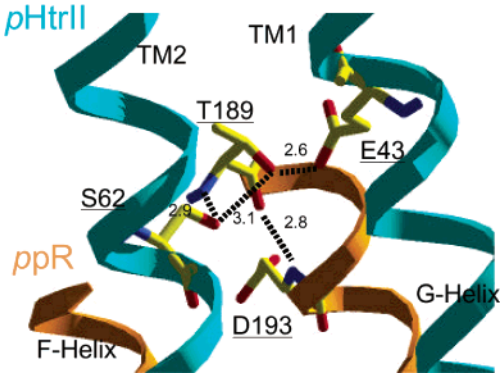


FIGURE 6: Possible explanation of why binding with *p*HtrII changes the p$K_a$ of Asp-193$^{ppR}$ and vice versa. The X-ray crystallographic structure of the region of Asp-193 and Thr-189 in the *p*pR/*p*HtrII complex is shown. Hydrogen bonds are inferred from the structure, and the numbers accompanying the bond (broken thick line) give the hydrogen-bonding distances in angstroms. The distance of the backbone between Thr-189$^{ppR}$ and Asp-193$^{ppR}$ is 2.8 Å, which permits the formation of a hydrogen bond. Thr-189$^{ppR}$ interacts with Ser-62$^{pHtrII}$ and Glu-43$^{pHtrII}$, so that the p$K_a$ of Asp-193$^{ppR}$ is affected by the binding. The membrane normal is roughly in the vertical plane of this figure, and the top and bottom regions correspond to the extracellular and cytoplasmic sides, respectively. The structure was obtained from the Protein Data Bank (PDB code 1H2S).

*Role of the Positively Charged Patch in the Interaction with pHtrII.* The substitution of Asp-214$^{ppR}$ did not significantly affect the $K_D$ value in the *p*pR$_{O-like}$ state. On the other hand, the mutant K157/R162/R164 (3Gln) showed an increased $K_D$ value (Table 2). This suggests that at least one of these residues is important for the interaction with *p*HtrII. Among these, we found that Arg-162 is a required residue for the interaction with *p*HtrII (manuscript in preparation). The side chain of Arg-162 extends toward transmembrane-2 (TM-2) of *p*HtrII. According to the crystal structure of *p*HtrII (*17*), no residue functions as an electrically interactive counterpart of the Arg-162 residue in TM-2 of *p*HtrII. Since the distance between Arg-162 of *p*pR and TM-2 of *p*HtrII is small, hydrophobic and/or van der Waals interactions may occur. Details regarding the Arg-162 may be clarified in the future.

## CONCLUDING REMARKS

In the present paper, we propose a role for Asp-193 during transducer binding in that the protonation/deprotonation state of Asp-193 affects the binding and vice versa. This may originate from the complicated intermolecular hydrogen-bonding network. This residue is important since it is a proton-releasing residue (*28*) and maintains the protein conformation (*43*) and its protonation induces Cl binding (*28*, *43*). Binding of *p*pR with *p*HtrII decreases the p$K_a$ of the carboxyl group of Asp-193$^{ppR}$, which inhibits $Cl^-$ binding. The effect of the protonation state of Asp-193$^{ppR}$ (e.g., comparison between Asp-193 and Asn-193) on phototaxis is an important question that should be examined. In addition, K157/R162/R164 contributes to complex binding.

## ACKNOWLEDGMENT

We thank M. Yamabi for invaluable discussion.

## REFERENCES

1. Imamoto, Y., Shichida, Y., Hirayama, J., Tomioka, H., Kamo, N., and Yoshizawa, T. (1992) Chromophore configuration of pharaonis phoborhodopsin and its isomerization on photon absorption, *Biochemistry 31*, 2523−2528.
2. Iwamoto, M., Kandori, H., and Kamo, N. (2003) Photochemical properties of pharaonis phoborhodopsin (sensory rhodopsin II), *Recent Res. Dev. Chem. 1*, 15−30.
3. Spudich, J. L. (2002) Spotlight on receptor/transducer interaction, *Nat. Struct. Biol. 9*, 797−799.
4. Pebay-Peyroula, E., Royant, A., Landau, E. M., and Navarro, J. (2002) Structural basis for sensory rhodopsin function, *Biochim. Biophys. Acta 1565*, 196−205.
5. Oesterhelt, D. (1998) The structure and mechanism of the family of retinal proteins from halophilic archaea, *Curr. Opin. Struct. Biol. 8*, 489−500.
6. Beja, O., Aravind, L., Koonin, E. V., Suzuki, M. T., Hadd, A., Nguyen, L. P., Jovanovich, S. B., Gates, C. M., Feldman, R. A., Spudich, J. L., Spudich, E. N., and DeLong, E. F. (2000) Bacterial rhodopsin: evidence for a new type of phototrophy in the sea, *Science 289*, 1902−1906.
7. Bieszke, J. A., Braun, E. L., Bean, L. E., Kang, S., Natvig, D. O., and Borkovich, K. A. (1999) The nop-1 gene of neurospora crassa encodes a seven transmembrane helix retinal-binding protein homologous to archaeal rhodopsins, *Proc. Nat.l Acad. Sci. U.S.A. 96*, 8034−8039.
8. Spudich, J. L., Yang, C.-S., Jung, K.-H., and Spudich, E. N. (2000) Retinylidene proteins: structures and functions from archaea to humans, *Annu. Rev. Cell. Biol. 16*, 365−392.
9. Lanyi, J. K., and Luecke, H. (2001) Bacteriorhodopsin, *Curr. Opin. Struct. Biol. 11*, 415−419.
10. Kamo, N., Shimono, K., Iwamoto, M., and Sudo, Y. (2001) Photochemistry and photoinduced proton-transfer by pharaonis phoborhodopsin, *Biochemistry (Moscow) 66*, 1277−1282.
11. Rudolph, J., Nordmann, B., Storch, K. F., Gruenberg, H., Rodewald, K., and Oesterhelt, D. (1996) A family of halobacterial transducer proteins, *FEMS Microbiol. Lett. 139*, 161−168.
12. Falke, J. J., Bass, R. B., Butler, S. L., Chervitz, S. A., and Danielson, M. A. (1997) The two-component signaling pathway of bacterial chemotaxis: a molecular view of signal transduction by receptors, kinases, and adaptation enzymes, *Annu. Rev. Cell Dev. Biol. 13*, 457−512.
13. Alley, M. R., Maddock, J. R., and Shapiro, L. (1993) Requirement of the carboxyl terminus of a bacterial chemoreceptor for its targeted proteolysis, *Science 259*, 1754−1757.
14. Maddock, J. R., and Shapiro, L. (1993) Polar location of the chemoreceptor complex in the *Escherichia coli* cell, *Science 259*, 1717−1723.
15. Rudolph, J., and Oesterhelt, D. (1996) Deletion analysis of the che operon in the archaeon *Halobacterium salinarium*, *J. Mol. Biol. 258*, 548−554.
16. Zhang, X. N., Zhu, J., and Spudich, J. L. (1999) The specificity of interaction of archaeal transducers with their cognate sensory rhodopsins is determined by their transmembrane helices, *Proc. Natl. Acad. Sci. U.S.A. 96*, 857−862.
17. Gordeliy, V. I., Labahn, J., Moukhametzianov, R., Efremov, R., Granzin, J., Schlesinger, R., Büldt, G., Savopol, T., Scheidig, A. J., Klare, J. P., and Engelhard, M. (2002) Molecular basis of transmembrane signalling by sensory rhodopsin II−transducer complex, *Nature 419*, 484−487.
18. Kandori, H., Tomioka, H., and Sasabe, H. (2002) Excited-state dynamics of pharaonis phoborhodopsin probed by femtosecond fluorescence spectroscopy, *J. Phys. Chem. A 106*, 2091−2095.
19. Yan, B., Takahashi, T., Johnson, R., and Spudich, J. L. (1991) Identification of signaling states of a sensory receptor by modulation of lifetimes of stimulus-induced conformations: the case of sensory rhodopsin II, *Biochemistry 30*, 10686−10692.
20. Ikeura, Y., Shimono, K., Iwamoto, M., Sudo, Y., and Kamo, N. (2003) Arg-72 of pharaonis phoborhodopsin (sensory rhodopsin II) is important for the maintenance of the protein structure in the solubilized state, *Photochem. Photobiol. 77*, 96−100.
21. Sudo, Y., Yamabi, M., Iwamoto, M., Shimono, K., and Kamo, N. (2003) Interaction of *Natronobacterium pharaonis* phoborhodopsin (sensory rhodopsin II) with its cognate transducer probed by increase in the thermal stability, *Photochem. Photobiol. 78*, 511−516.
22. Shimono, K., Iwamoto, M., Sumi, M., and Kamo, N. (1997) Functional expression of *pharaonis* phoborhodopsin in *Escherichia coli*, *FEBS Lett. 420*, 54−56.
23. Sudo, Y., Iwamoto, M., Shimono, K., and Kamo, N. (2001) *pharaonis* phoborhodopsin binds to its cognate truncated trans-

ducer even in the presence of a detergent with a 1:1 stoichiometry, *Photochem. Photobiol. 74*, 489−494.
24. Sudo, Y., Iwamoto, M., Shimono, K., and Kamo, N. (2002) Association between a photo-intermediate of a M-lacking mutant D75N of pharaonis phoborhodopsin and its cognate transducer, *J. Photochem. Photobiol., B 67*, 171−176.
25. Sudo, Y., Iwamoto, M., Shimono, K., and Kamo, N. (2002) Tyr-199 and charged residues of pharaonis Phoborhodopsin are important for the interaction with its transducer, *Biophys. J. 83*, 427−432.
26. Sudo, Y., Furutani, Y., Shimono, K., Kamo, N., and Kandori, H. (2003) Hydrogen bonding alteration of Thr-204 in the complex between *pharaonis* phoborhodopsin and its transducer Protein, *Biochemistry 42*, 14166−14172.
27. Royant, A., Nollert, P., Edman, K., Neutze, R., Landau, E. M., Pebay-Peyroula, E., and Navarro, J. (2001) X-ray structure of sensory rhodopsin II at 2.1-A resolution, *Proc. Natl. Acad. Sci. U.S.A. 98*, 10131−10136.
28. Iwamoto, M., Hasegawa, C., Sudo, Y., Shimono, K., and Kamo, N. (2004) Proton release and uptake of pharaonis phoborhodopsin (sensory rhodopsin II) reconstituted into phospholipid, *Biochemistry 40*, 3195−3203.
29. Dioumaev, A. K., Richter, H. T., Brown, L. S., Tanio, M., Tuzi, S., Saito, H., Kimura, Y., Needleman, R., and Lanyi, J. K. (1998) Existence of a proton-transfer chain in bacteriorhodopsin: participation of Glu-194 in the release of protons to the extracellular surface, *Biochemistry 37*, 2496−2509.
30. Brown, L. S., Sasaki, J., Kandori, H., Maeda, A., Needleman, R., and Lanyi, J. K. (1995) Glutamic acid 204 is the terminal proton release group at the extracellular surface of bacteriorhodopsin, *J. Biol. Chem. 278*, 36556−36562.
31. Balashov, S. P., Imasheva, E. S., Ebrey, T. G., Chen, N., Menick, D. R., and Crouch, R. K. (1997) Glutamate-194 to cysteine mutation inhibits fast light-induced proton release in bacteriorhodopsin, *Biochemistry 36*, 8671−8679.
32. Seidel, R., Scharf, B., Gautel, M., Kleine, K., Oesterhelt, D., and Engelhard, M. (1995) The primary structure of sensory rhodopsin II: a member of an additional retinal protein subgroup is coexpressed with its transducer, the halobacterial transducer of rhodopsin II, *Proc. Natl. Acad. Sci. U.S.A. 92*, 3036−3040.
33. Essen, L. O., Siegert, R., Lehmann, W. D., and Oesterhelt, D. (1998) Lipid patches in membrane protein oligomers: crystal structure of the bacteriorhodopsin-lipid complex, *Proc. Natl. Acad. Sci. U.S.A. 95*, 11673−11678.
34. Iwamoto, M., Sudo, Y., Shimono, K., and Kamo, N. (2001) Selective reaction of hydroxylamine with chromophore during the photocycle of pharaonis phoborhodopsin, *Biochim. Biophys. Acta 1514*, 152−158.
35. Hippler-Mreyen, S., Klare, J. P., Wegener, A. A., Seidel, R., Herrmann, C., Schmies, G., Nagel, G., Bamberg, E., and Engelhard, M. (2003) Probing the sensory rhodopsin II: Binding domain of its cognate transducer by calorimetry and electrophysiology, *J. Mol. Biol. 330*, 1203−1213.
36. Kandori, H., Shimono, K., Sudo, Y., Iwamoto, M., Shichida, Y., and Kamo, N. (2001) Structural changes of *pharaonis* phoborhodopsin upon photoisomerization of the retinal chromophore: Infrared spectral comparison with bacteriorhodopsin, *Biochemistry 40*, 9238−9246.
37. Sudo, Y., Iwamoto, M., Shimono, K., and Kamo, N. (2002) Association of pharaonis phoborhodopsin with its cognate transducer decreases the photo-dependent reactivity by water-soluble reagents of azide and hydroxylamine, *Biochim. Biophys. Acta 1558*, 63−69.
38. Miyazaki, M., Hirayama, J., Hayakawa, M., and Kamo, N. (1992) Flash photolysis study on pharaonis phoborhodopsin from a haloalkaliphilic bacterium (*Natronobacterium pharaonis*), *Biochim. Biophys. Acta 1140*, 22−29.
39. Schmies, G., Lüttenberg, B., Chizhov, I., Engelhard, M., Becker, A., and Bamberg, E. (2000) Sensory rhodopsin II from the haloalkaliphilic *Natronobacterium pharaonis*: light-activated proton-transfer reactions, *Biophys. J. 78*, 967−976.
40. Furutani, Y., Iwamoto, M., Shimono, K., Kamo, N., and Kandori, H. (2002) FTIR Spectroscopy of the M Photointermediate in pharaonis Phoborhodopsin, *Biophys. J. 83*, 3482−3489.
41. Hein, M., Wegener, A. A., Engelhard, M., and Siebert, F. (2003) Time-Resolved FTIR Studies of Sensory Rhodopsin II (NpSRII) from *Natronobacterium pharaonis*: Implications for Proton Transport and Receptor Activation, *Biophys. J. 84*, 1208−1217.
42. Bergo, V., Spudich, E. N., Spudich, J. L., and Rothschild, K. J. (2003) Conformational Changes Detected in a Sensory Rhodopsin II-Transducer Complex, *J. Biol. Chem. 278*, 36556−36562.
43. Iwamoto, M., Furutani, Y., Sudo, Y., Shimono, K., Kandori, H., and Kamo, N. (2002) Role of Asp193 in chromophore-protein interaction of pharaonis phoborhodopsin (sensory rhodopsin II), *Biophys. J. 83*, 1130−1135.

BI048803C